On the influence of thermal hysteresis on the performance of thermomagnetic motors

C. V. X. Bessa,[1,a)] L. D. R. Ferreira,[1] O. Horikawa,[1] J. C. B. Monteiro,[2] F. G. Gandra,[2] and S. Gama[3]
[1]*Escola Politécnica of the University of São Paulo-EPUSP, São Paulo 05508-010, Brazil*
[2]*IFGW-University of Campinas-UNICAMP, Campinas, São Paulo 13083-970, Brazil*
[3]*Federal University of São Paulo-UNIFESP, Diadema, São Paulo 09910-720, Brazil*

(Received 24 October 2017; accepted 4 December 2017; published online 22 December 2017)

Although thermal hysteresis might be a problem in the magnetocaloric refrigeration, the same is not necessarily true for thermomagnetic motor applications. This work presents a comparison of the magnetocaloric properties of materials with first order magnetic transition (having large or narrow thermal hysteresis) to those with second order magnetic transition, assessing the application of these materials in thermomagnetic motors through a thermodynamic approach. Results show that the larger the thermal hysteresis, the higher the specific work produced in a thermal cycle. This allows operation at higher temperature differences with high efficiency relative to Carnot efficiency, when compared with systems using narrow hysteresis and second order transition materials. *Published by AIP Publishing*. https://doi.org/10.1063/1.5010356

I. INTRODUCTION

First order magnetic transitions (FOMTs) are associated with structural transitions and in these cases, the magnetocaloric effect is much higher than the strictly magnetic effect.[1] Due to this, a FOMT is normally accompanied by thermal hysteresis,[2] giving rise to problems in magnetocaloric refrigeration, causing losses in the cooling cycles. In the worst case, a too large hysteresis may nullify the magnetocaloric effect in a large range of magnetic fields,[3,4] making unfeasible the application of many materials in magnetic refrigeration.

However, the same does not happen with thermomagnetic motors, in which the operational temperature is not determined by the temperature change due to the magnetocaloric effect as in magnetic refrigerators. As long as the temperature difference between sources is high enough to surpass thermal hysteresis, the thermomagnetic motor is capable of producing work.

Houston and Thomson published the first idea of a thermomagnetic motor in 1879.[5,6] However, the most famous thermomagnetic motors were those patented by Edison[7] and Tesla.[8] Figure 1 shows a thermomagnetic motor based on Tesla's patent. The magnetocaloric material (MCM) is initially cold, in a ferromagnetic (FM) state, in contact with the heat sink, as shown in Fig. 1(a). The magnetic field gradient provided by the permanent magnet array (composed by the permanent magnets and the soft magnetic material) attracts the MCM to the high magnetic field region, compressing the spring and placing the MCM in contact with the heat source. At this moment, the MCM begins to warm up under constant magnetic field. The MCM magnetization decreases due to the thermomagnetic effect,[9] then the magnetic force experienced by the MCM dramatically reduces when it reaches the paramagnetic (PM) state. Now, the compressed spring pushes the MCM toward the heat sink, as shown in Fig. 1(b). The MCM is brought back into contact with the heat sink, and it begins to cool under a constant and very low magnetic field. The MCM magnetization increases as its temperature decreases, becomes FM, returns to the initial state shown in Fig. 1(a), and thus, the motor completes a cycle of operation.

It is possible to note that the MCM heating and cooling processes happen under constant magnetic field. Considering that the MCM does not exchange heat during the displacement between the heat sink and the heat source, the MCM suffers two isofield and two adiabatic processes, therefore describing a Brayton cycle. The produced work can be extracted from this motor using the work output piston that is linked to the MCM [Fig. 1(b)].

This study describes the behavior of thermomagnetic motors that operate under a Brayton cycle for different materials, investigating how the thermal hysteresis changes and contributes to the theoretical work and efficiency of these machines using a thermodynamic approach.

II. BRAYTON CYCLE OF THERMOMAGNETIC MOTORS AND MATERIAL PROPERTIES

Thermomagnetic motors as the one described in Fig. 1 operate in a Brayton cycle, in a reverse sense of the magnetocaloric refrigerators, as shown in previous works using the T-s (temperature–entropy) diagrams.[9–13] In order to apply the thermodynamic cycle approach to these motors, it is necessary to know the MCM entropy as a function of the temperature for different applied magnetic fields. By determining the specific heat of the MCM, it is possible to calculate the specific entropy change (s-s_0) using

$$s(T,H) - s_0 = \int_{T_0}^{T} \frac{C_H}{T} dT \Big|_H . \quad (1)$$

H is the applied magnetic field, C_H is the apparent specific heat at constant pressure and applied magnetic field,

[a)]Author to whom correspondence should be addressed: carlosviniciusxb@usp.br

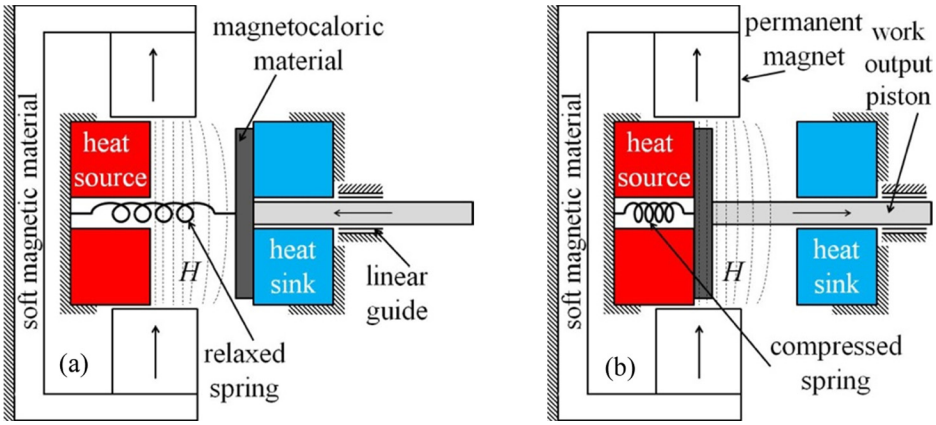

FIG. 1. Thermomagnetic motor based on Tesla's patent.[8] (a) MCM in contact with the heat sink. (b) MCM in contact with the heat source. H is the applied magnetic field.

and T is the temperature. The sub-index 0 indicates the initial value.[4]

The specific heat curves obtained during the heating and the cooling processes show different behaviors in materials with FOMT due to the thermal hysteresis (ΔT_{Hys}). Thus the entropy curves also show different behaviors for each process. A large hysteresis implies a large difference between the entropy curves during the heating and the cooling processes. The magnetic field shifts the transition temperature and changes the behavior of the specific heat, as shown in Fig. 2(a) for a MnAs powder sample under magnetic fields of 0 T and 1.5 T (a magnetic field level attainable with permanent magnets arrays[14,15]). ΔT_B is the peak temperature shift caused by the magnetic field during heating. This temperature marks the end of the magnetic transition associated with the structural transition. The curves were obtained using a device described by Monteiro *et al.*[16,17] by measuring the heat flow ($\dot{Q}$) to maintain a constant heating or cooling temperature rate ($\dot{T}$) in the MCM sample with mass m. The C_H is calculated by

$$C_H = \frac{\dot{Q}(T,H)}{m.\dot{T}}. \tag{2}$$

This way, the apparent specific heat includes the specific heat and the latent heat contribution during the structural transition of a FOMT material. Figure 2(b) shows the entropy changes as a function of the temperature calculated using Eq. (1).

In Tesla type thermomagnetic motors, the heating of the material happens under high magnetic field and the cooling under low magnetic field. To ensure the transition between FM and PM states using FOMT materials in a machine operating between 0 T and 1.5 T, the heat sink temperature (T_{Cold}) has to be lower than the transition temperature during the cooling process at 0 T. Also, the heat source temperature (T_{Hot}) has to be higher than the transition temperature during the heating process at 1.5 T. Considering the described conditions, the corresponding Brayton cycle of the thermomagnetic motor is shown in gray in Fig. 2(b).

The thermomagnetic motor specific work produced in a cycle (w) can be calculated by

$$w = \int_{s_2}^{s_3} Tds\Big|_{H=1.5T} - \int_{s_1}^{s_4} Tds\Big|_{H=0T}. \tag{3}$$

Considering that the magnetic material reaches the thermal steady state, equalizing its temperature with the heat source in the heating process and with the heat sink in the cooling process, the amount of heat necessary in the heating process (q_{Hot}) is defined by

$$q_{Hot} = \int_{T_2}^{T_3} C_H dT\Big|_{H=1.5T}. \tag{4}$$

The efficiency (η) and the efficiency relative to the Carnot efficiency (η_{rel}) can be calculated by

$$\eta = \frac{w}{q_{Hot}}, \tag{5}$$

$$\eta_{rel} = \frac{\eta}{1 - \frac{T_{Cold}}{T_{Hot}}}. \tag{6}$$

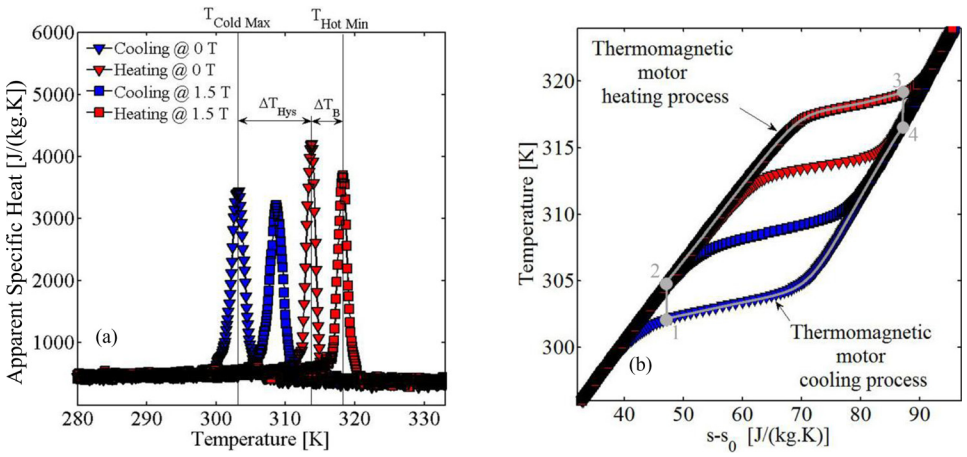

FIG. 2. (a) MnAs specific heat during the heating and cooling for magnetic fields of 0 T and 1.5 T. (b) MnAs entropy changes calculated using Eq. (1) and $T(s_0) = 276$ K. A Brayton cycle with heating process at 1.5 T (2 to 3) and cooling process at 0 T (4 to 1) in gray.

TABLE I. Temperature conditions used in the Brayton cycles construction, and ΔT_{Hys} and ΔT_B for each studied material.

Material	$T_{ColdMax}$ (K)	T_{HotMin} (K)	T_{HotMin}- $T_{ColdMax}$ (K)	ΔT_{Hys} (K)	ΔT_B (K)	Reference
Gd	293	293	0	0	…	Risser *et al.*[19]
$LaFe_{11.22}Mn_{0.46}Si_{1.32}H_{1.65}$	269.5	276.5	7	~0	6.8	Basso *et al.*[20]
$LaFe_{11.76}Mn_{0.06}Si_{1.18}H_{1.65}$	338.2	344.2	6	1.5	4.8	Basso *et al.*[20]
$Mn_{1.3}Fe_{0.65}P_{0.5}Si_{0.5}$	272.8	278.9	6.1	1	5.1	Bartok *et al.*[21]
MnAs	303.2	318.3	15.1	10.6	4.5	This work

Sub-indexes 1, 2, 3, and 4 are the MCM thermodynamic states shown in Fig. 2(b).

One can verify the influence of the thermal hysteresis on the work produced by the thermomagnetic motors by comparing the MnAs (a material of large hysteresis) with other magnetic materials. Gd is adopted as a benchmark material (second order magnetic transition—SOMT material). Brayton cycles are built regarding the temperature conditions that ensure the transition between the FM and PM states for each FOMT material. Also, the generated work and the efficiency per cycle are verified for each material. Since Gd does not suffer a structural transition during its magnetic transition, ΔT_{Hys} is zero and ΔT_B does not exist. In the SOMT cases, the magnetic transition happens in a smooth way, having a large temperature range around the Curie temperature where the magnetization changes. Due to that, it is even possible to operate a thermomagnetic motor with the MCM only in the FM state using SOMT materials.[18] The Curie temperature of Gd is used as a reference to build Brayton cycles for the SOMT work and efficiency calculations. Table I shows the studied materials and temperatures conditions. $T_{ColdMax}$ is the maximum value of the heat sink temperature and T_{HotMin} is the minimal value of the heat source temperature that ensure the magnetic transition in a heating process at magnetic field of 1.5 T and cooling process at 0 T for the FOMT materials. In the SOMT analysis, it is assumed that $T_{ColdMax}$ and T_{HotMin} are equal to the MCM Curie temperature. Figure 3 shows the T-s diagrams for each material where the Brayton cycles were built.

III. RESULTS AND DISCUSSION

In all the studied materials, a higher applied temperature difference produced larger specific work However, there is a limit for the work produced per cycle when the increase of the temperature difference between the hot and cold sources does not change the specific work, and this limit is different for each material. For temperatures intervals far from the transition, the specific work does not change when the temperature difference increases. This happens because the influence of the magnetic field on the specific heat is very small, far from the Curie temperature, making the T-s curves superimposed for different applied magnetic fields in this condition. Far from the transition, all heat provided by the heat source is rejected to the cold source, and no work is obtained. Figures 4(a)–4(c) present the specific work as a function of the temperature of the heat sink and the heat source for Gd, $LaFe_{11.76}Mn_{0.06}Si_{1.18}H_{1.65}$, and MnAs, respectively. There is a clear difference between the work produced by a FOMT and a SOMT material. In the second order transition, the minimal specific work is zero, and this happens when

$$T_{Hot} = T_{Cold} + \Delta T_{ad}. \tag{7}$$

ΔT_{ad} is the temperature change due to the magnetocaloric effect in an adiabatic magnetic field change. FOMT materials showed a minimal specific work higher than zero. Materials with FOMT store thermal energy due to compound effect of ΔT_{Hys} and ΔT_B before the transition. Part of the stored energy is converted into work when the transition happens. Thus, the minimal specific work produced in a thermomagnetic motor will happen when $T_{Cold} = T_{ColdMax}$ and $T_{Hot} = T_{HotMin}$, provided that $T_{Cold} + \Delta T_{ad} < T_{Hot}$.

The MnAs (material with the largest thermal hysteresis among the studied materials) shows the largest specific work and it is more than twice of the one produced by $LaFe_{11.76}Mn_{0.06}Si_{1.18}H_{1.65}$. Among the studied FOMT materials, this compound was the second in terms of ΔT_{Hys} and specific work when the saturation of specific work is reached. The MnAs also shows the largest minimum specific work, and it is greater than the maximum specific work expected for the other FOMT materials. Figure 4(d) shows the specific work as a function of the difference of the heat source and the heat sink temperatures, when T_{Cold} is 2 K below the $T_{ColdMax}$ for each material. For the same temperature difference, the specific work using MnAs can be almost 4.5 times larger than that by using Gd. The thermal

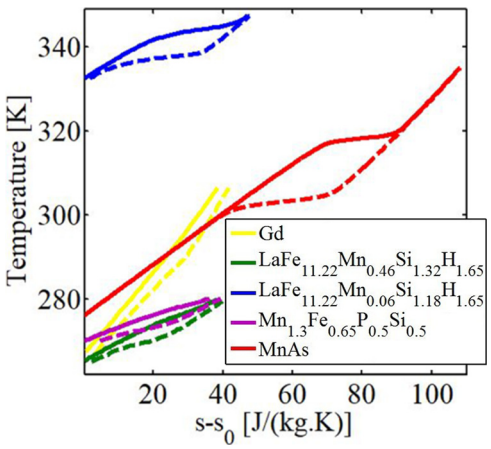

FIG. 3. Temperature as a function of the specific entropy calculated using Eq. (1) for the studied thermomagnetic materials. Dashed lines: cooling at 0 T field; solid lines: heating at 1.5 T field. Gd: calculated from C_H data of Risser *et al.*,[19] $T(s_0) = 270$ K. $LaFe_{11.22}Mn_{0.46}Si_{1.32}H_{1.65}$ and $LaFe_{11.76}Mn_{0.06}Si_{1.18}H_{1.65}$: s-$s_0$ data from Basso *et al.*[20] $Mn_{1.3}Fe_{0.65}P_{0.5}Si_{0.5}$: s-$s_0$ data from Bartok *et al.*[21] MnAs: calculated from C_H data of this work, $T(s_0) = 276$ K.

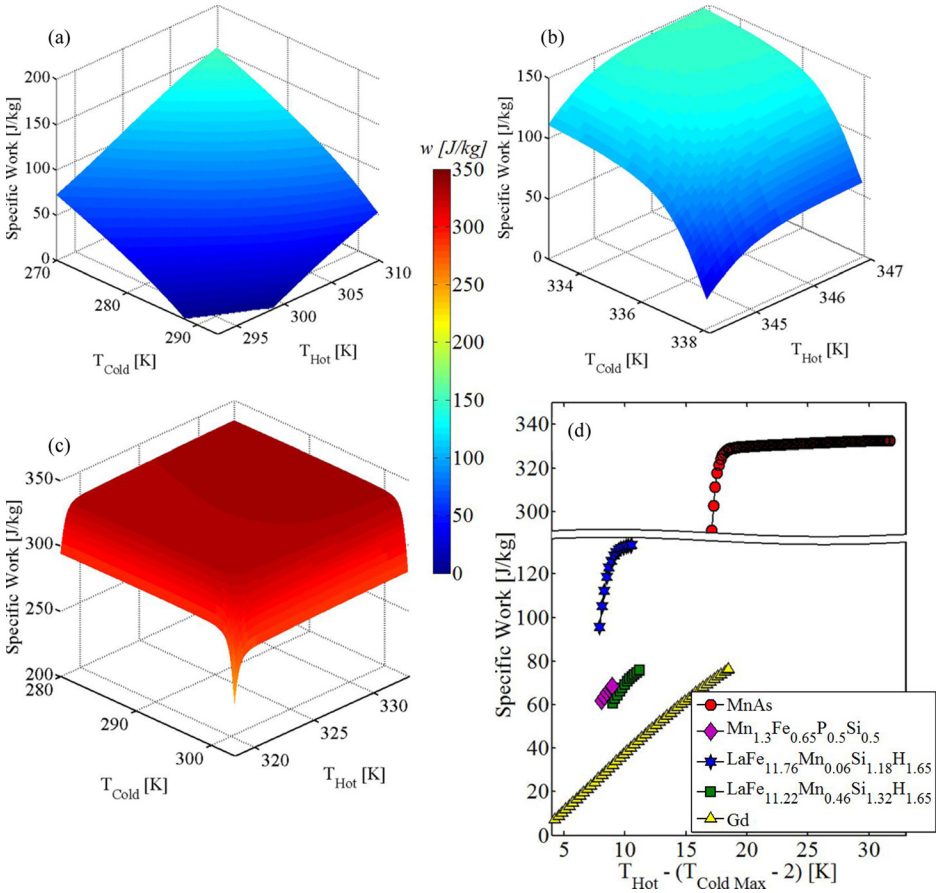

FIG. 4. Specific work as a function of the heat sink and heat source temperatures: (a) Gd, (b) $LaFe_{11.76}Mn_{0.06}Si_{1.18}H_{1.65}$, and (c) MnAs. (d) Specific work when the heat sink temperature is 2 K below the $T_{Cold\ Max}$.

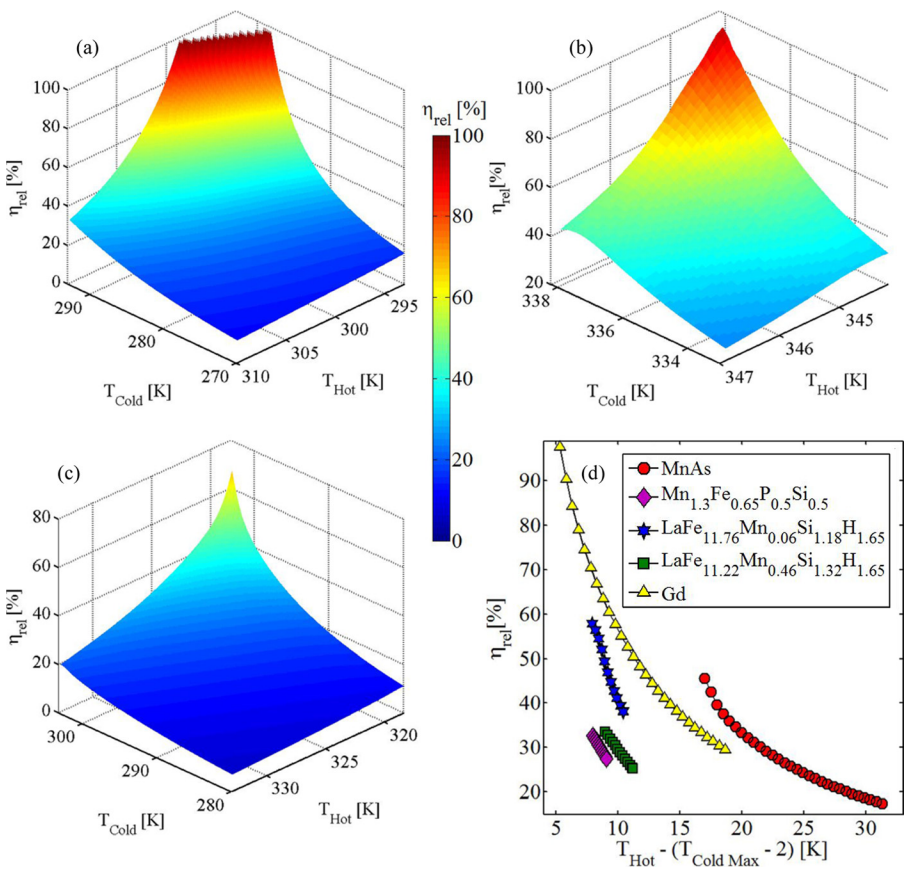

FIG. 5. Efficiency relative to Carnot efficiency as a function of the heat sink and heat source temperatures: (a) Gd, (b) $LaFe_{11.76}Mn_{0.06}Si_{1.18}H_{1.65}$, and (c) MnAs. (d) Efficiency relative to Carnot efficiency when the heat sink temperature is 2 K below the $T_{Cold\ Max}$.

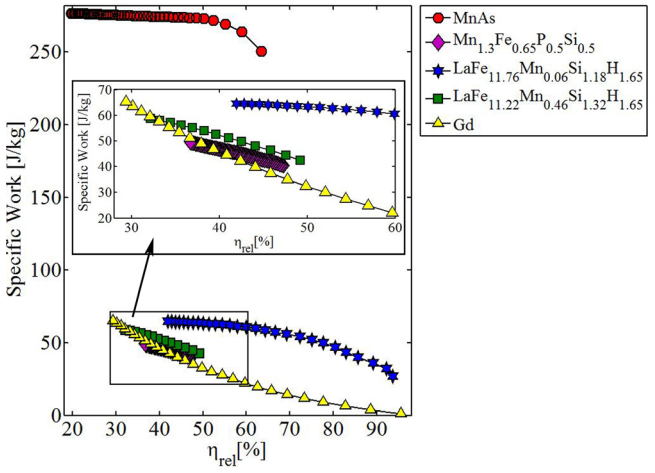

FIG. 6. Specific work as a function of the efficiency relative to Carnot efficiency when the heat sink temperature is $T_{ColdMax}$.

hysteresis increases the separation between the curves of the heating and cooling processes in the T-s diagram, increasing the area equivalent to the work in the Brayton cycle. This way, the large hysteresis implies a high specific work production.

When Eq. (7) is valid, the efficiency approaches Carnot efficiency. However it rapidly decreases when the temperature difference between the heat sink and the heat source increases. The maximal η_{rel} is reached in the condition of minimal specific work. Figures 5(a)–5(c) present the efficiency relative to Carnot efficiency as a function of the heat sink and heat source temperatures, for Gd, $LaFe_{11.76}Mn_{0.06}Si_{1.18}H_{1.65}$ and MnAs, respectively. Figure 5(d) shows the η_{rel} for the same condition presented in Fig. 4(d). In the MnAs, the large thermal hysteresis allows applications of higher temperature differences without a strong reduction in the η_{rel}. Wide ΔT_{Hys} materials enable the application of thermomagnetic motors in higher temperature differences when compared with motors using materials with narrow thermal hysteresis or SOMT, increasing the motors' energetic density without affecting the efficiency.

Among the studied materials, those that show the best relation between the specific work and the efficiency relative to Carnot efficiency are the materials with larger thermal hysteresis. Figure 6 shows the specific work as function of the η_{rel} when $T_{Cold} = T_{ColdMax}$. As it has the largest thermal hysteresis, MnAs presents the best performance followed by the compound $LaFe_{11.76}Mn_{0.06}Si_{1.18}H_{1.65}$ in the entire range where the materials produce work. The materials with hysteresis equal to or lower than 1 K show a behavior similar to the Gd.

IV. CONCLUSIONS

The thermal hysteresis increases the separation between the heating and the cooling curves in the temperature-entropy diagram. As a consequence, thermomagnetic motors using magnetic materials with large thermal hysteresis show higher specific work than motors using materials with narrow or null thermal hysteresis. If the hysteresis is large, a significant amount of thermal energy is accumulated in the material before the ferromagnetic to paramagnetic transition, and part of this thermal energy is converted into work. In this case, high thermal energy storage implies a high work production. The large thermal hysteresis also allows the application of thermomagnetic motors in conditions of higher temperature differences, with higher energetic density without affecting the efficiency relative to Carnot efficiency when compared with motors using second order magnetic transitions and narrow thermal hysteresis materials.

ACKNOWLEDGMENTS

The *Fundação de Amparo à Pesquisa do Estado de São Paulo* (FAPESP) Grant No. 2015/26799-0 supported this work. The authors also thank the *Conselho Nacional de Desenvolvimento Científico e Tecnológico* (CNPq). This work is dedicated to Professor Isaías da Silva.

[1]L. Tocado, E. Palacios, and R. Burriel, J. Appl. Phys. **105**, 093918 (2009).
[2]J. L. Zhao, J. Shen, F. X. Hu, Y. X. Li, J. R. Sun, and B. G. Shen, J. Appl. Phys. **107**, 113911 (2010).
[3]L. Von Moos, K. K. Nielsen, K. Engelbrecht, and C. R. H. Bahl, Int. J. Refrig. **37**, 303 (2014).
[4]L. Tocado, E. Palacios, and R. Burriel, J. Therm. Anal. Calorim. **84**, 213 (2006).
[5]E. J. Houston and E. Thomson, J. Franklin Inst. **107**, 39 (1879).
[6]C. Hering, J. Franklin Inst. **124**, 278 (1887).
[7]T. A. Edison, U. S. patent US380100 A (27 March 1888).
[8]N. Tesla, U. S. patent US396121 A (15 January 1889).
[9]D. Solomon, J. Appl. Phys. **65**, 3687 (1989).
[10]K. N. Andreevski, A. G. Mandzhavidze, I. G. Margvelashvili, and S. V. Sobolevskaya, Tech. Phys. **43**, 3687 (1998).
[11]P. W. Egolf, A. Kitanovski, M. Diebold, C. Gonin, and D. Vuarnoz, J. Magn. Magn. Mater. **321**, 758 (2009).
[12]D. Vuarnoz, A. Kitanovski, C. Gonin, Y. Borgeaud, M. Delessert, M. Meinen, and P. W. Egolf, Appl. Energy **100**, 229 (2012).
[13]M. Almanza, A. Pasko, F. Mazaleyrat, and M. LoBue, IEEE Trans. Magn. **53**, 2502106 (2017).
[14]C. Vasile and C. Muller, Int. J. Refrig. **29**, 1318 (2006).
[15]R. Bjork, C. R. H. Bahl, A. Smith, and N. Pryds, Int. J. Refrig. **33**, 437 (2010).
[16]J. C. B. Monteiro, R. D. Reis, M. Mansanares, and F. G. Gandra, Appl. Phys. Lett. **105**, 74104 (2014).
[17]J. C. B. Monteiro, F. C. G. Gandra, and N. R. Dilley, "Determination of the magnetocaloric properties using a PPMS," Quantum Design Application Note 1085-200 (2014); available at https://www.qdusa.com/sitedocs/appNotes/ppms/1085-200.pdf.
[18]Y. Takahashi, K. Yamamoto, and M. Nishikawa, Electr. Eng. Jpn. **154**, 68 (2006).
[19]M. Risser, C. Vasile, B. Keith, T. Engel, and C. Muller, Int. J. Refrig. **35**, 459 (2012).
[20]V. Basso, M. Küpferling, C. Curcio, C. Bennati, A. Barzca, M. Katter, M. Bratko, E. Lovell, J. Turcaud, and L. F. Cohen, J. Appl. Phys. **118**, 53907 (2015).
[21]A. Bartok, M. Kuepferling, C. Curcio, V. Basso, A. Pasko, K. Z. L. Bessais, F. Mazalerat, and M. LoBue, in *Proceedings of the Refrigeration Science and Technology (Thermag VII)* (International Institute of Refrigeration, Torino, 2016), pp. 119–122.